PROCEEDINGS OF THE IV INTERNATIONAL CONFERENCE/HIGH TEMPERATURE CAPILLARITY

JOURNAL OF MATERIALS SCIENCE **40** (2005) 2437–2441

Influence of wettability on bubble formation in liquid

S. GNYLOSKURENKO*
IIS, The University of Tokyo, 4-6-1 Komaba, Meguro-ku, Tokyo, 153-8505, Japan
E-mail: slava@iis.u-tokyo.ac.jp

A. BYAKOVA
IPM, Ukrainian National Academy of Sciences, 3 Krzhyzhanivs'ky St., 03142 Kyiv, Ukraine

T. NAKAMURA
IMRAM, Tohoku University, 2-1-1 Katahira, Aoba-ku, Sendai 980-8577, Japan

O. RAYCHENKO
IPM, Ukrainian National Academy of Sciences, 3 Krzhyzhanivs'ky St., 03142 Kyiv, Ukraine

This paper presents experimental results of the surface phenomena effect on bubble formation from a single orifice in water and at nozzle in liquid aluminium with gas blowing at small flow rates. The usage of coated orifice in water and nozzles of different materials in the melt realized wide range of contact angles. The meaningful stages, termed (1) nucleation period, (2) under critical growth, (3) critical growth and (4) necking, were identified during bubble formation in a regime referring to simultaneous forced flow and surface tension control. It was revealed that bubble formation is substantially dominated by hysteresis of contact angle. Evolution of interface equilibrium and force balance conditions distinctive for bubble formation is clarified. X-ray fluoroscope was used to carry out *in-situ* observation of bubble formation in the melt. It was shown that bubble volume increased with wettability worsening both for aqueous and metallic systems. A further insight into the mechanism of the bubble formation was obtained by comparison of the bubble behaviour at the tip of the injection devices in liquid aluminium and at the orifice in water.

1. Introduction

The size of bubbles plays an important role in various processes involved dispersions of gas bubbles in liquids. Although bubble formation in aqueous and metallic systems is considered to be extremely complicated phenomenon a number of single-stage or two-stage models [1–14] have been developed for description of bubble growth and prediction of its volume. The general outline relates to the geometrical assumptions concerning the spherical or hemispherical shape of the bubble [1, 3, 4].

Close prediction of experimental results under high flow rate conditions has been seen, even though the theoretical models developed are different in concept [3, 4, 7]. However, the discrepancies between theoretical prediction and experimental results could be illustrated by extension of these models on bubble formation at lower flow rates. Since the surface tension force is the dominating factor at these conditions it is reasonable to conclude that these discrepancies occur due to the influence of surface phenomena on bubble formation.

A few studies in liquid metal showed too that wettability of nozzles plays an important role in bubble growth [15–17]. These authors observed that the outer diameter of non-wetted nozzles controls the bubble size in liquid mercury, silver, and iron.

The evidences above indicate that bubble growth mechanism at varying wettabilty especially that in high temperature melts is still unclear.

This paper aims to study experimentally bubble formation mechanism and volume at detachment at a single orifice in water as well as at the free standing nozzle in liquid aluminium under low gas flow rate and wide range of wetting contact angles.

2. Experimental procedure

The apparatus used in this study (Fig. 1 [18]) consists of a clear container filled with water, an orifice block of acrylic plastic with hole (diameter 1 mm) submerged to a depth of 24 mm, air delivery, measuring and controlling systems.

Gas was blown through orifice at flow rate of 1–5 cm^3/min and high speed CCD camera recorded the bubble formation process. Every bubble image was divided into regular geometrical parts to calculate the

*Author to whom all correspondence should be addressed.

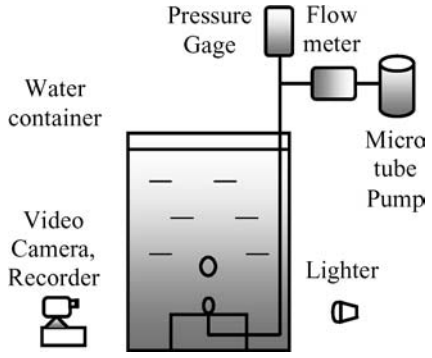

Figure 1 Schematic view of the experimental set up for bubble formation study in water.

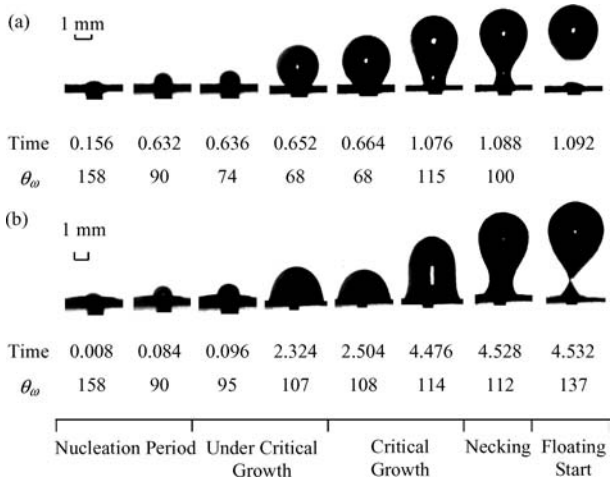

Figure 2 Bubble growth at the orifice during all stages up to floating start. The time is shown in seconds. θ_ω—current contact angle, degree: (a) good wettability ($\theta_o = 68^\circ$) and (b) poor wettability ($\theta_o = 110^\circ$).

volume and surface area of each bubble. Measurement data were much precise than assumption of the previous researchers for bubble to have either spherical [19] or ellipsoidal [7] shapes.

To vary wetting conditions the orifice plate was coated by vacuum silicon grease (referred as "good wettability", $\theta_o = 68^\circ < 90^\circ$, where θ_o is a contact angle, formed with water drop at equilibrium on the smooth substrate) or paraffin provided "poor wettability", $\theta_o = 110^\circ > 90^\circ$. Pure acrylic plastic performed "neutral wettability", $\theta_o = 90^\circ$.

Bubble formation at the nozzle in aluminium melt was studied with the X-ray system of 150 kV source, described in [20]. The nozzles facing upward with inner diameter, $D_i = 0.1$–0.4 cm and outer one, $D_o = 0.2$–1.0 cm were used to inject argon into the melt. Injection devices were connected to gas cylinder via flow rate controller and pressure gauge.

The nozzles were made of steel, silica and alumina to establish different wettability by liquid aluminium with reference to rough values of the contact angle in high-temperature melt. Since iron is perfectly wetted by aluminium ($\theta_o \ll 90^\circ$) [21] and $\theta_o \approx 33^\circ$ [22] low carbon steel was chosen to perform good wettability as well as alumina nozzle leads to poor wettability, $\theta_o \approx 120^\circ > 90^\circ$ [23, 24]. Authors [25] reported the contact angle for SiO_2 in liquid Al to decrease from 150° to 90° with time and temperature increase, whereas Kaptay [26] indicated that $\theta_o = 50$–60°. So, wettability of silica nozzle is considered here to be neutral, i.e., better than that of alumina and poorer than that of steel.

At the melt temperature of 690°C the injection device was preheated and introduced into the melt while argon gas blowing. Flow rate was increased step by step from 0.43 to 12 cm^3/s and X-ray observation was carried out for 30 s at every constant flow rate.

The frequency of bubble formation, f was visually evaluated by counting the number of bubbles generated at the nozzle exit on video tape. The bubble volume V_b was then determined by using equation $V_b = Q/f$, where Q is the gas flow rate, cm^3/s.

3. Results and discussion

3.1. Mechanism of bubble formation in water

Fig. 2 shows the sequence of bubble formation in the vicinity of the orifice in water. The main periods of bubble evolution, bubble nucleation at the initiation and bubble growth including several meaningful stages such as under critical growth, critical growth and necking, which extends up to bubble floating start could be distinguished. Although the mechanism of bubble evolution is similar regardless to wetting conditions, differences in bubble shape, volume, growth kinetics during each period and stage are revealed. Attention should be also drawn to the fact that bubble forms under conditions when contact angle hysteresis is happened.

During nucleation bubble emerges from the capillary in form of a spherical segment, transforms into part of sphere while its periphery remains constant and causes contact angle hysteresis referred to static case. Receded contact angle, $\theta_R = \theta_\omega$, decreases and at the end of the period reaches $\approx 90^\circ$ regardless to the initial wetting conditions (Fig. 2).

During under critical growth bubble configuration remains part of sphere-like at the good and neutral wettability whereas at poor wettability it is likely spherical segment at the tip. The bubble expands greatly while its base moves lengthways the plate away from the orifice lip, allowing the dynamic case of contact angle hysteresis. At good and poor wettability receding contact angle takes the equilibrium value ($\theta_\omega = \theta_R = \theta_0$) when the widening of bubble periphery stops at the end of the stage. At neutral wetting conditions θ_ω holds the constancy during the all stage and it does not differ from equilibrium value ($\theta_\omega = \theta_o = 90^\circ$).

Previous study has shown [18] that the force balance in the direction of bubble detachment is attained during the stage following undercritical growth and the interface equilibrium at the triple line is disturbed. From this point of view this stage is the most important one and referred here as critical growth. During this stage the bubble becomes elongated, expands while moving upwards and substantial distortion of bubble configuration in comparison with spherical or hemispherical shape occurs. The bubble volume increases significantly with the inversion of an air-water interface displacement. However, bubble periphery at the base maintains a stable value, allowing the static case of

contact angle hysteresis. Regardless to the initial wetting conditions advanced contact angle increases at the end of the stage, attaining values $\theta_0 < \theta_\omega = \theta_A > 90^o$.

During last necking stage the spherical tip moves continually upwards. Share of bubble spherical part increases significantly, resulting in great progress of spheroidization process. Moreover, contact angle hysteresis of dynamic nature happens since bubble periphery moves continually toward the orifice due to weakening the impressed drive. Finally, the bubble detachment starts at the neck cross-section and bubble travels away from the orifice remaining a small volume of gas (not exceed 1% of bubble volume detached) on the orifice.

The study shows that the difference in wettability caused difference in both bubble volume and the time of its evolution that increased with equilibrium contact angle. Hysteresis referred to forced displacement of the interface dominates on bubble periphery behaviour. Static hysteresis occurred during nucleation period and at the stage of critical growth whereas that of dynamic case happened during stages of under critical growth and necking. Thus, at extremely low flow rates surface phenomena at the orifice plate control the bubble periphery dimension, the bubble configuration and making the bubble volume dependent on its geometrical parameters.

Despite of this a number of currently accepted theoretical models consider that as the flow rate tends to zero the bubble volume V at force balance is assumed to be independent on geometrical parameters and is to be determined by the equating the buoyancy force, $V\Delta\rho g$ with the surface tension force, $2\pi r_o \cos\theta$ as in the "drop weight" method (where r_o is an orifice radius) [1, 3, 4, 27].

Unlike that in the previous models the experiments published in [28] have proved that the theory given originally by Kabanov and Frumkin [29] for stable stationary bubble could be valuable to describe adequately bubble formation in the regime referring to simultaneous forced flow and surface tension control when flow rate is extremely small ($\sim$1–5 cm^3/min). Taking into account bubble geometrical parameters such as radius at the tip R_o, height H, bubble periphery D and maximum value of current contact angle θ_ω at hysteresis, the concept of Kabanov and Frumkin, gives that there are various forces acting on the bubble: (i) Upward buoyancy force ($V\Delta\rho g$), (ii) Downward adhesive force that occurs in response to vertical component of surface tension force ($\pi D\sigma_{LG}\sin\theta_\omega$) (iii) Force due to Laplace's pressure, acting upwards ($\pi D^2\sigma_{LG}/2R_o$), and (iv) Force due to hydrostatic pressure gradient along the bubble height H, acting downwards ($\pi D^2\rho g H/4$).

By comparison of the experimental results and theoretical approach of Kabanov and Frumkin [29] evolution of the interface equilibrium and force balance conditions could be surveyed. The analysis indicates that interface equilibrium at the triple line takes place only once in the instance at the start of bubble critical growth stage. Unlike that in previous models the balance between upward and downward forces takes place periodically at the critical points, i.e. at the end of nucleation period and at the end of the critical growth stage. During periods of under critical growth, critical growth and slight necking stage the bubble formation is dominated by the downward forces, which are greater than the upward forces. The last overcome the former at the bubble detachment.

Thus, the present study allows understanding the reasons caused the discrepancies between theoretical predictions of the models and experimental results at the extremely small flow rate. Firstly the discrepancies can occur due to the considerable difference in geometrical assumptions accepted by these models and experimental shapes of the bubbles. The second reason is that the bubble formation occurred in four stages rather than in single or two stages accepted by the models. Additionally, the disagreement on force balance conditions accepted by models [1–7, 12, 13, 27] and those assigned above may contribute directly in these discrepancies.

Indeed, one can think that the different geometrical assumptions accepted by the theoretical models are made due to different flow conditions. However, it is reasonable to assume that the degradation process of bubble evolution arises in response to gradually increasing gas flows when the effect of surface phenomena becomes negligible. It results in reducing stages and modes assigned above for bubble formation up to the disappearance of some of them.

3.2. Bubble formation at the nozzle in liquid aluminium

The results of bubble formation study in liquid aluminium are presented in Figs 3–5. Volume of the bubble issued from the nozzle of steel, silica and alumina with equal inner diameter (D_i = 1 mm) and different outer ones (D_o = 2 and 10 mm) is plotted vs. gas flow rate in Fig. 3. Alumina nozzle produced much large bubbles (0.7–1.0 cm^3 for D_o = 10 mm) that nozzles of steel and silica did (0.5–0.6 cm^3). It confirms that nozzle of poor wettability results in larger bubble. Injection devices with D_o = 10 mm formed much larger bubbles than nozzles of 2 mm. Thus it may be concluded that bubbles detached from the outer circumference for all non-wetted nozzles. Tip of the steel nozzles supposed to be wetted by molten aluminium was probably partly

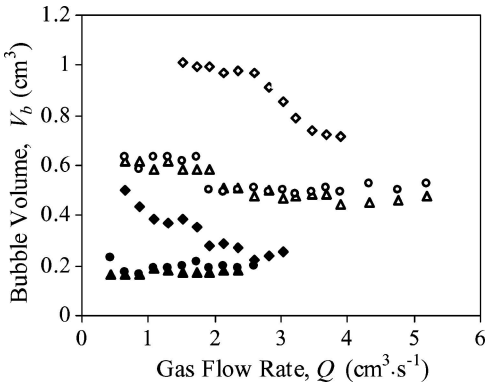

Figure 3 Bubble volume—gas flow rate dependence for nozzles of steel, silica and alumina in liquid aluminium. Outer diameter is varied (D_o = 2 or 10 mm) and inner diameter is constant (D_i = 1 mm).

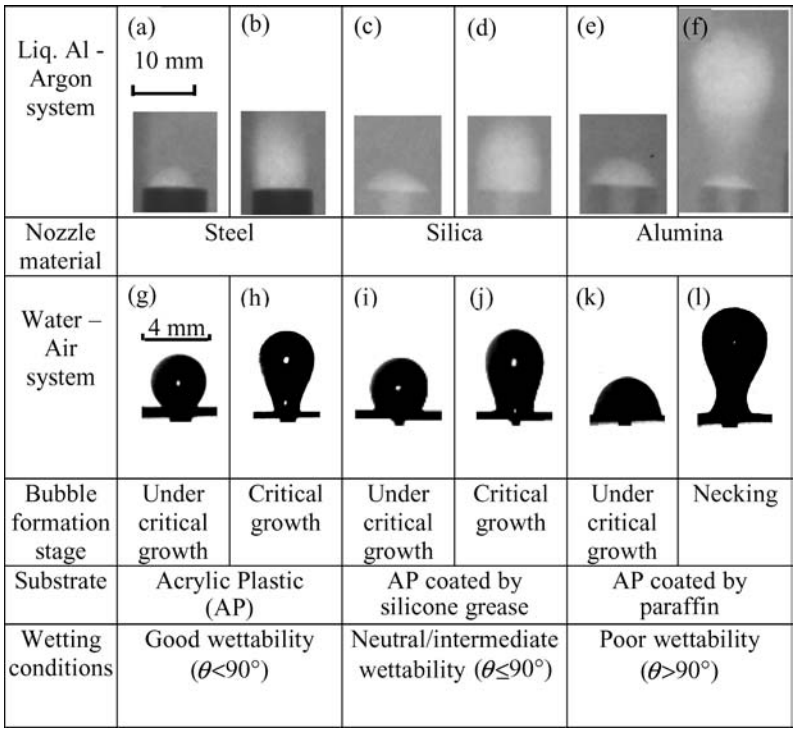

Figure 4 Bubble evolution on the tip of the injection devices (1 mm in diameter of the hole) of different wettability in the melt a–f and in the aqueous system g–l.

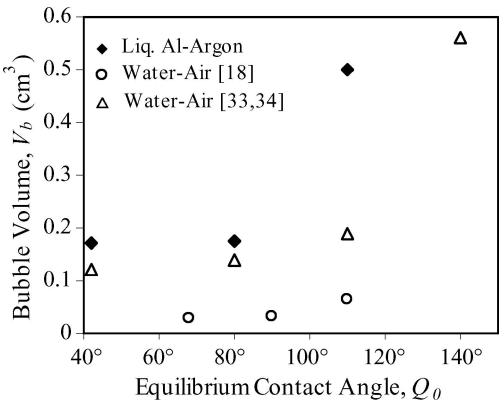

Figure 5 Dependence of bubble volume, V_b on equilibrium contact angle, θ_0 in Liquid Aluminum—Argon and Water-Air [18, 33, 34] systems. Q—gas flow rate, inner diameter of the injection hole, $D_i = 1$ mm.

oxidized while preheating in the furnace, which caused wettability worsening. Therefore, bubble was not fixed around injection hole but most likely spreaded over oxidized steel tip to some extends that results in bubble volume comparative to that produced from silica nozzle (Fig. 3).

In situ observation allows comparing mechanism of bubble formation on the tip of injection devices (1 mm in hole diameter) of different wettability in the melt (Fig. 4a–f) and in the aqueous system (Fig. 4g–l). Although the surface tension of molten aluminium and water are different ($\sigma_{water} = 72.37 \times 10^{-3}$ Nm^{-1} and $\sigma_{Al} = 860 \times 10^{-3}$ Nm^{-1}) the experiments were carried out at the same range of contact angles (similar wetting conditions), which include those typical for metallurgical processes. Moreover very low gas flow rate employed here ensured regime of predominance of the surface forces in bubble formation for the both systems. It is also important to note that orifice surface in water had almost unlimited area for bubble spreading whereas nozzle in the melt was confined with the outer diameter.

Similar stages of bubble evolution were revealed, named under critical growth, critical growth and necking. In water every stage depicted in the Fig. 4g–k concern the end of the corresponding stages from Fig. 2. After arising from the hole gas spread to a limited extend over the wetted tip of steel and acrylic plastic (Fig. 4a and g), whereas it covered larger adherence area over non-wetting surface (Fig. 4e and k) being at the intermediate position under neutral wetting (Fig. 4c and k). After spreading bubble base was fixed in the position between outer and inner diameter of the steel nozzle (Fig. 4a and b). The larger adherence area was the more extended time was needed to establish conditions for bubble detachment from a nozzle (force balance). During this period bubble was supplied with an additional gas with increase in the bubble volume at detachment. The bubble further grew only upward in the melt (Fig. 4b and d) as happened during critical growth stage in water (Fig. 4h and j) when bubble shape deformed and became elongated. Similar bubble behaviour and shape was also observed in aqueous system [11, 29–31] and mercury [32]. During the last stage the neck formation began (Fig. 4f and l shown here only for non wetted systems) and final bubble volume formed under poor wetting conditions was found to be much larger than that under good wettability. So, at very low gas flow rate bubbles formed over the solid surface in liquid aluminium and water in similar way under predominant effect of wettability.

Fig. 5 shows the dependence of the bubble volume on contact angle in liquid aluminium and water [18, 33, 34]. Experimental bubble volume in metallic

system is presented for the lowest gas flow rates ($Q = 0.648\ cm^3 \cdot s^{-1}$) used in the present study. It was determined that bubble volume increased as contact angle increased both for aqueous and metallic systems. Apparently, bubbles formed in water [18] are one order of magnitude smaller (0.03–0.06 cm^3) than that in liquid aluminium (0.17–0.49 cm^3). This can be mainly attributed to the significant difference in surface forces taking place in aqueous and metallic systems and gas flow rates applied for bubble formation study. Data of Mukai *et al.* for aqueous system [33, 34] (Fig. 5) confirms that increase in gas flow rate up to 10 cm^3/s resulted in bubble volume increase and fitted the data to that of the present metallic system.

4. Conclusion

Bubble formation at an orifice in water and at the free-standing nozzle in liquid aluminium has been studied at small gas flow rate and a wide range of contact angles. Two significant periods, i.e. nucleations at the initiation and growth period have been revealed during bubble evolution at the orifice. Under critical growth, critical growth and necking have been assigned as meaningful stages of the bubble growth period.

Contact angle hysteresis revealed while forcing the triple line of contact due to gas injection was considered to dominate on bubble periphery behaviour and, so, on bubble formation. The substantial distortion of bubble configuration in comparison with spherical or hemispherical shape, which increased with an increase of equilibrium contact angle, has been observed at the critical growth stage. Experimental observation allowed to compare bubble formation with assumption accepted by the theoretical models.

X-ray examination of bubble formation in liquid aluminium using nozzles of different material showed the influence of wettability on bubble volume and evolution similar to that observed in aqueous system. It was shown that bubble volume increased with contact angle both for aqueous and metallic systems. Similar stages of bubble evolution were revealed. The present study showed that injection devices wetted by liquid melt are reasonable to use, particularly in metal foaming techniques, for producing small bubbles in the melt.

References

1. R.-Q. LI and R. HARRIS, *Can. Metall. Q.* **32** (1993) 31.
2. J. F. DAVIDSON, A. M. I. MECH and B. O. G. SHULER, *Trans. Inst. Chem. Eng.* **38** (1960) 144.
3. *Idem.*, *ibid.* **38** (1960) 335.
4. R. KUMAR and N. R. KULOOR, *Chem. Tech.* **19** (1967) 733.
5. S. RAMAKRISHNAN, R. KUMAR and N. R. KULOOR, *Chem. Eng. Sci.* **24** (1969) 731.
6. R. KUMAR and N. R. KULOOR, *Adv. Chem. Eng.* **8** (1970) 256.
7. A. E. WRAITH, *Chem. Eng. Sci.* **26** (1971) 1659.
8. A. MARMUR and E. RUBIN, *ibid.* **31** (1976) 453.
9. M. SANO and K. MORI, *Trans. JIM* **17** (1976) 344.
10. D. A. DESHPANDE, M. D. DEO, F. V. HANSON and A. G. OBLAD, *Chem. Eng. Sci.* **47** (1992) 1669.
11. W. FRITZ, *Pysik. Z.* **36** (1935) 379.
12. R. D. LANAUZE and I. J. HARRIS, *Chem. Eng. Sci.* **29** (1974) 1663.
13. *Idem.*, *ibid.* **27** (1972) 2012.
14. B. D. SUMM and YU. V. GORYUNOV, "Phisico-Chemical Fundamentals of Wetting and Spreading" (Chemistry Publisher, Moscow, 1976) (in Russian).
15. M. SANO and K. MORI, *Trans. JIM* **17** (1976) 344.
16. G. A. IRONS and I. L. GUTHRIE, *Metall. Trans.* **9B** (1978) 101.
17. K. OKUMURA, R. HARRIS and M. SANO, *Can. Metall. Q.* **37** (1998) 49.
18. S. V. GNYLOSKURENKO, A. V. BYAKOVA, O. I. RAYCHENKO and T. NAKAMURA, *Colloids Surf. A* **218** (2003) 73.
19. L. DAVIDSON and E. H. AMICK, *A.I.Ch.E. J.* **2** (1956) 337.
20. S. V. GNYLOSKURENKO and T. NAKAMURA, *Materials Transactions* **44**(11) (2003) 2298.
21. YU. V. NAYDICH, "Contact Phenomena in Metallic Melts" (Naukova Dumka, Kiev, 1972) p. 196 (in Russian).
22. V. N. EREMENKO, T. S. IVANOVA and N. D. LESNIK, *Adhesion Melts Weld. Mater.* **6** (1980) 51 (in Russian).
23. B. M. GALLOIS, *JOM* June (1997) 48.
24. V. LAURENT, D. CHATAIN, C. CHATILLON and N. EUSTATHOPOULOS, *Acta Metall.* **36** (1988) 1797.
25. V. LAURENT, D. CHATAIN and N. EUSTATHOPOULOS, *Mater. Sci. Eng.* **A135** (1991) 89.
26. G. KAPTAY, in "Metal Foams and Porous Metal Structure," edited by J. Banhart, M. F. Ashby and N. A. Fleck (MIT-Verlag, Bremen, 1999) p. 141.
27. A. SATYANARAYAN, R. KUMAR and N. KULOOR, *Chem. Eng. Sci.* **24** (1969) 749.
28. A. V. BYAKOVA, S. V. GNYLOSKURENKO, T. NAKAMURA and O. I. RAYCHENKO, *Colloids Surf. A* **229** (2003) 19.
29. B. KABANOV and A. FRUMKIN, *Z. Physik. Chem. (A), Band* **165** (1933) 433.
30. I. W. WARK, *J. Physic. Chem.* **37** (1933) 623.
31. Y. MIZUNO and M. IGUCHI, *ISIJ Int.* **41** (2001) S56.
32. H. TERASHIMA, T. NAKAMURA, K. MUKAI and D. IZU, *J. Japan Inst. Metals* **56** (1992) 422.
33. K. MUKAI, H. NOZAKI and T. ARIKAWA, *CAMP ISIJ* **3** (1990) 137.
34. K. MUKAI, *ISIJ Int.* **32** (1992) 19.

Received 31 March
and accepted 18 July 2004